LWT - Food Science and Technology 250 (2026) 119500

Contents lists available at ScienceDirect

LWT

journal homepage: www.elsevier.com/locate/lwt

Active chitosan films containing *Zingiber officinale* Roscoe essential oil for *Aspergillus flavus* inhibition and peanut butter preservation

Yiming Zhang [a], Qian Li [a,*], Fred Mwabulili [a], Hongying Xiao [a], Jianhua Wang [b,**]

[a] Henan Key Laboratory of Cereal and Oil Food Safety and Nutrition, College of Food Science and Engineering, Henan University of Technology, Zhengzhou, China
[b] Institute for Agri-food Standards and Testing Technology, Shanghai Academy of Agricultural Sciences, Shanghai, China

ARTICLE INFO

Keywords:
Peanut butter
Zingiber Officinale Roscoe
essential oil
Composite film
Lipid oxidation
Protein oxidation

ABSTRACT

Peanut butter, particularly homemade varieties lacking antioxidants, is highly susceptible to oxidation, posing risks during processing, storage, and consumption. To address this, this study developed a novel chitosan film incorporated with *Zingiber officinale* Roscoe essential oil (GEO) to evaluate its antifungal properties and impact on peanut butter preservation. Results demonstrated that GEO acted as a potent inhibitor against *Aspergillus flavus* with a minimum inhibitory concentration of 8 μL/mL. Additionally, the antioxidant activity of the composite films increased with higher GEO concentrations. Physical assessments revealed these films possessed greater thickness and moisture content, alongside reduced water solubility and swelling compared to controls. The films' preservation efficacy was tested on peanut butter stored at 40 °C for 21 days. The composite films effectively maintained texture properties, closely matching the hardness, cohesiveness, and gumminess of fresh peanut butter, while delaying adhesiveness increases. Furthermore, treatments with the highest GEO concentration significantly alleviated lipid and protein oxidation. This was evidenced by minimal increases in peroxide, acid, thiobarbituric acid values, and carbonyl content, alongside unchanged fatty acid and amino acid compositions, and stable protein electrophoresis band intensities. Sensory evaluations confirmed excellent overall acceptability comparable to fresh samples, proving this non-contact preservation method highly promising.

1. Introduction

As a popular sauce-based snack, the production and consumption of peanut butter is huge worldwide. According to the data in a market analysis and forecast report, China's peanut butter output was approximately 1.1 million tons in 2026 (IndexBox, 2026). In the United States, approximately 1.25 million metric tons of peanuts were utilized for producing peanut butter in 2024 (Liu et al., 2025). From 2021 to 2027, the global peanut butter market is expected to maintain an annual growth rate of 4% to 10% (Sithole et al., 2022). Overweight adolescents consuming peanut butter snacks on a daily basis exhibit a significant decrease in their Body Mass Index (BMI) after 6 months as it can effectively regulate appetite and therefore reduce the intake of high-calorie snacks (Moreno, 2015).

However, high-fat and high-protein can be a double-edged sword. Peanut butter, for example, is easily to be contaminated by *Aspergillus flavus* (*A. flavus*) and oxidized when exposed to air. Firstly, *A. flavus* is a ubiquitous saprophytic fungus found in soil, dust, air, etc. Fresh prepared peanut butter provides a desirable medium for the colonization and germination of *A. flavus* spores. Meanwhile, a more serious problem is aflatoxins. Even the fungi are killed; the accumulated prior biosynthesized aflatoxins can still threaten food safety. Adolescents and children are the population at the highest risk of exposure, and chronic AF exposure may increase the risk of liver cancer (Knutsen et al., 2018). Still, proactive controlling strategies (restraining spore germination) have proved to be effective in suppressing aflatoxin production, especially in food storage and processing.

Secondly, the oxidation of peanut butter usually leads deterioration of quality (inferior mouthfeel, unpleasant odor, and darkened color), safety risks (elevated peroxide value and acid value), and nutrition (vitamins and antioxidants) losses, rendering peanut butter unfit for consumption (Liu et al., 2025). Generally, the oxidation involves a synergistic mechanism between lipid peroxidation and protein oxidation. Upon inter- and outer circumstances, the dominated monounsaturated fatty acid-oleic acid and polyunsaturated fatty acids-linoleic acid both serve as primary targets of lipid oxidation through

* Corresponding author.
** Corresponding author.
E-mail addresses: lq@haut.edu.cn (Q. Li), jianhuawang163@163.com (J. Wang).

https://doi.org/10.1016/j.lwt.2026.119500
Received 15 January 2026; Received in revised form 23 April 2026; Accepted 10 May 2026
Available online 14 May 2026

auto-oxidation, photo-oxidation, and enzymatic oxidation (Schaich, 2014). Followed by lipid oxidation, the oxidized products (e.g. hydroperoxides, malondialdehyde (MDA), 4-hydroxy-2-nonenal, and acrolein, etc.) subsequently initiate protein oxidation through radical attacks (Geng et al., 2023). To mitigate these oxidation problems, manufacturers usually employ natural alternatives (vitamin C, vitamin E) or permitted synthetic antioxidants (e.g. butylated hydroxytoluene and butylated hydroxyanisole) (Brewer, 2011), as well as atmosphere modified packaging (Mungalpara et al., 2025). However, such strategies either occasionally trigger consumers' concerns about the potential health risks, even though the additive levels meet national standards, or increase the production costs.

Plant essential oil is a complex blend of volatile, small molecular compounds naturally present in plants. As many of them possess varied bioactive activities, such as antioxidative, antimicrobial, insect-repellent, without posing harm to human health or the environment, they have been extensively proposed as natural food preservatives (Burt, 2004). Among them, *Zingiber Officinale* Roscoe (ginger) essential oil (GEO) has recently garnered significant attention in the food industry. Modern food research has extensively demonstrated the exceptional broad-spectrum and antioxidant capabilities of GEO. Specifically, GEO has proven highly effective against foodborne pathogens and severe spoilage fungi, including *A. flavus* (Nerilo et al., 2020), *Fusarium verticillioides* (Yamamoto-Ribeiro et al., 2013), and *Pseudomonas aeruginosa* (Septama et al., 2023). Consequently, the latest applications of GEO have been continuously expanding in food preservation, significantly extending the shelf life of duck breast (Chen et al., 2024), cheese (Vitalini et al., 2022), and tofu (Hamad et al., 2023).

Although the direct incorporation of GEO into food matrices yields desirable preservation effects, its high volatility and intense, pungent aroma present inevitable challenges. Rapid volatilization diminishes its long-term efficacy, while the strong inherent flavor can easily mask or alter the sensory profile of delicate foods like peanut butter. To circumvent these limitations, recent technological advancements have shifted toward encapsulating essential oils into biopolymer matrices, such as starch, gelatin, and chitosan, to formulate active packaging microcapsules or films (Calderón-Oliver & Ponce-Alquicira, 2022; Sultan et al., 2023).

Particularly, chitosan, a polycationic biopolymer naturally derived from marine chitin, is highly favored for active food packaging due to its excellent film-forming ability, tunable gas permeability, and intrinsic antimicrobial properties (Sana et al., 2025; Shetta et al., 2024). Recently, the development of chitosan-GEO composite films has emerged as a research hotspot. For instance, montmorillonite/chitosan membranes incorporated with GEO as a wrapping package reduced the amount of several pathogens, including *Bacillus cereus*, *Staphylococcus aureus* (*S. aureus*), *Salmonella Typhimurium* (*S. Typhimurium*), *Escherichia coli* (*E. coli*), etc., while retarding lipid oxidation in meat (Souza et al., 2018). More recently, chitosan-GEO coatings have been successfully employed to maintain the postharvest freshness of plums for up to 35 days (Showkat et al., 2025).

Despite these promising advancements, a critical research gap remains. The application of chitosan-GEO composite films has predominantly relied on direct-contact methods (e.g., wrapping meat or coating fruits). For high-fat, semi-solid products like nut spreads, direct contact is often impractical and exacerbates unwanted flavor migration. To the best of our knowledge, utilizing chitosan-GEO films in a non-contact (active headspace) manner to synchronously inhibit *A. flavus* and retard the synergistic lipid-protein oxidation in peanut butter has not yet been explored.

Therefore, in the present work, we prepared chitosan-GEO composite films, and conducted (1) non-contact antifungal test of chitosan-GEO against *A. flavus* in culture medium and on peanut butter; (2) influence of chitosan-GEO on the quality (texture properties, lipid oxidation, protein oxidation, sensory evaluation, etc.) of peanut butter during storage. This study offers a practical approach for developing a composite film for home storage and/or alternative processing strategy of peanut butter, and uncovers the key mechanism by which the film inhibits lipid co-oxidation of proteins in semi-solid foods.

2. Materials and methods

2.1. Extraction of GEO

The extraction process was conducted as described previously (Nerilo et al., 2015). Fresh gingers were bought from the local supermarket. After washing, the gingers were cut into about 3 mm thin slices, baked in an 80 °C electric blast drying oven for 8 h. Afterward, the slices were crushed into powder. Fifty g of ginger powder was added with 1 L of distilled water, and then ultrasonic-assisted extraction (600 W, 25 °C for 1 h) was conducted. GEO was extracted for 6 h in a steam distillation unit (SZCL-2, Gongyi Yuhua Instrument Co., Ltd., Gongyi, China). The extraction rate of GEO was determined through the method outlined below:

$$\text{Extraction rate } (\%) = \frac{g_2}{g_1} \times 100$$

Where g_1 is the weight of the extracted dried ginger powder, and g_2 is the weight of the extracted GEO.

2.2. Chemical analysis of GEO

The composition of GEO was assessed through GC-MS (Agilent 7890A/5975C, Agilent Technologies Co., Ltd., California, USA), the chromatographic column was an Agilent HP-5MS UI capillary column (40 m × 0.25 mm, 0.25 μm). Dissolve 100 μL of GEO in methanol to a final capacity of 5 mL followed by filtration. The programme was as follows: the temperature was maintained at 70 °C for 3 min, then increased to 150 °C at a heating rate of 5 °C/min and held for 3 min. The temperature was then further raised to 154 °C at a rate of 0.5 °C/min and held for 2 min, followed by an increase to 240 °C at a rate of 25 °C/min, and maintained for 4 min. Helium was used as the carrier gas; the flow rate was 1 μL/min and the constant pressure was 228 kPa.

2.3. Antifungal activity of GEO in vitro

A. flavus was bought from the China General Microbiological Culture Collection Center (CGMCC). The fungus was cultured on Sabouraud Dextrose Agar (SDA) at 28 ± 2 °C for one week. The medium contained 4% glucose, 1% peptone, and 2% agar. The antifungal test was conducted as Li et al. (2021) described. In brief, GEO was mixed with SDA medium and carefully poured into a sterile Petri dish, and the mixture culture medium was called as SDA-GEO plate. The final concentrations of GEO were 0, 2, 4, 6, 8, and 10 μL/mL. After cultivating *A. flavus* on SDA for 7 days, fungal discs with a diameter of 6 mm were excised and inoculated onto SDA-GEO plates. The inhibition rate of mycelial growth was determined through the method outlined below:

$$\text{Inhibition rate } (\%) = \frac{d_1\text{-}d_2}{d_1} \times 100$$

Where d_1 represents the mycelial growth diameter of the control group (without GEO) minus 6 mm, and d_2 denotes the mycelial growth diameter in the GEO treatment group minus 6 mm. The diameter of mycelial growth was measured every 24 h, and the MIC was determined to be the minimum GEO concentration that completely suppressed fungal growth after 3 days.

2.4. Fabrication of the composite film

The chitosan film was prepared following the previously outlined method with minor adjustments (Wang et al., 2020). To prepare a 2%

chitosan solution, chitosan was mixed with a 1% glacial acetic acid solution and stirred continuously in a 40 °C water bath until fully dissolved. After adding glycerol (0.03% w/v), the solution was stirred for another 2 h. Subsequently, 0, 0.4, 0.8, and 1.6% (v/v) of GEO, along with Tween 80 (0.2%, v/v), were incorporated, followed by another 2 h of stirring. The resulting film solution (10 mL) was cast into circular molds with a 7 cm diameter and subsequently dried at 40 °C for a duration of 24 h to obtain chitosan, C-GEO1, C-GEO2, and C-GEO3 films, corresponding to the afore-mentioned concentrations of GEO. The films were then sealed in a desiccator before experiments.

2.5. Physical parameters of the film

2.5.1. Thickness, swelling index, and water solubility

The film thickness was assessed with a digital micrometer (211-101K, Shanghai Sanliang Tools Co., Ltd., Shanghai, China).Measurement methods for swelling index and water solubility were adapted from the protocols established by Akyuz and Riaz (Akyuz et al., 2018; Riaz et al., 2018), with slight modifications. Soak the dried film in 100 mL of distilled water for a duration of 24 h. Afterward, remove the film and gently absorb excess water on the surface. Subsequently, weigh the film, and the swelling index was calculated using the following formula:

$$\text{Swelling index } (\%) = \frac{W_2\text{-}W_1}{W_1} \times 100$$

In this context, W_1 represents the weight of the film after drying, while W_2 represents the weight of the film after being soaked.

Subsequently, dry the soaked film at 40 °C until the weight reached a stable value. The calculation formula was:

$$\text{Water solubility } (\%) = \frac{W_1\text{-}W_3}{W_1} \times 100$$

Where W_3 is the weight of the film after it dried.

2.5.2. Moisture content

The moisture content was assessed based on the experimental procedure established by Zhang et al. (2020). The film was subjected to drying in an oven at 105 °C for 24 h, and then weighed. The formula for calculating moisture content was as follows:

$$\text{Moisture content } (\%) = \frac{W_a\text{-}W_b}{W_b} \times 100$$

Where W_a and W_b refer to the mass of the film prior and after baking, respectively.

2.6. Antioxidant activity

The DPPH and ABTS radical scavenging activities of the composite were evaluated following the method outlined by Zhu et al. (2022). One gram of the film was combined with 10 mL of ethanol and stirred at 150 rpm and 25 °C for 3 h. Afterward, the mixture was filtered and centrifuged (8000 rpm, 4 °C, 10 min), and the supernatant was collected for further analysis. A 0.1 mM DPPH solution in methanol was prepared, and 1 mL of the film extract was mixed with an equal volume of the DPPH solution. The reaction mixture was kept at room temperature in the dark for 1 h, and the absorbance was measured at 517 nm. For the control group, ethanol without film extract was used. The calculation method was as follows:

$$\text{DPPH radical scavenging activity } (\%) = \frac{Abs_{Control}\text{-}Abs_{Sample}}{Abs_{DPPH}} \times 100$$

For the ABTS assay, equal volumes of a 7 mM ABTS solution and a 2.45 mM potassium persulfate solution were mixed and left to react overnight at 4 °C. The absorbance of the resulting solution was adjusted to 0.70 ± 0.02 at 734 nm with ethanol. Then, 1 mg of the film extract was combined with 1 mg of the ABTS solution, after reaction in the dark for 5 min, the absorbance was measured at 734 nm. The calculation method was as follows:

$$\text{ABTS radical scavenging activity } (\%) = \frac{Abs_{Control}\text{-}Abs_{Sample}}{Abs_{Control}} \times 100$$

2.7. Determination of peanut butter composition

The preparation process for peanut butter was conducted as previously described with minor adjustments (Gong et al., 2018). About 100 g of peanut kernels were baked for 13 min in an oven (T1-108B, Midea Group, Foshan, China) at 200 °C. After removing the peels, peanut kernels were ground with a grinder (BJ-300, Deqing Baijie Electric Co., Ltd., Huzhou, China). The nutritional composition of peanut butter was analyzed following AOAC guidelines.

2.8. Non-contact of C-GEO composite films against A. flavus on peanut butter

Non-contact antifungal activity assay was performed as previously described with slight modifications (Balaguer et al., 2013). Approximately 10 g of peanut butter was placed in a Petri dish (6.0 cm diameter) and sterilized with UV light for 30 min. Following sterilization, 150 μL of *A. flavus* spore suspension (5×10^5 spores/mL) was added on the peanut butter. Chitosan films, along with C-GEO1, C-GEO2, and C-GEO3, were affixed on the inner surface of the lid of the Petri dish, while a group without a film served as the control. The growth of *A. flavus* was observed every 24 h for 72h.

2.9. Effect of C-GEO on storage quality of peanut butter

2.9.1. Determination of pH value, color, and texture parameters

The peanut butter was stored at 40 °C for 21 days, and the pH value, color, and texture were measured every 3 days. The pH value of the peanut butter was assessed using the procedure outlined by Silva et al. (2017). Two grams of peanut butter was mixed with 20 mL of distilled water and stirred for 20 min before measuring with a pH meter (PHS-3C, Zhengzhou Baojing Electronic Technology Co., Ltd., Zhengzhou, China).

The color of the peanut butter was evaluated based on the method described by Saricaoglu and Turhan (2019). Ten grams of the sample were placed in a Petri dish with a 4 cm diameter. The color value of the sample was determined using a portable colorimeter (Sasaki Company, Tokyo, Japan).

The texture of the peanut butter was evaluated following the approach outlined by Huang et al. (2020). Fifty grams of peanut butter were added to a beaker (with a diameter of 4.5 cm and a height of 6 cm) with the surface smoothed. A texture analyzer fitted with a 1 kg load cell and a cylindrical probe (0.5 cm wide) was used to measure the texture parameters of the peanut butter. A downward force of 5 N was applied at a rate of 5 mm/s to penetrate the peanut butter by 2 cm, after which the probe was completely retracted. The texture parameters of the peanut butter were analyzed based on the force-deformation curve.

2.9.2. Lipid oxidation and total phenolic content of peanut butter

The PV of peanut butter was measured in accordance with the method specified in Chinese National Standard GB 5009.227-2016.

$$\text{PV } (g/100g) = \frac{(V\text{-}V_0) \times C \times 0.126 \times 100}{m}$$

Where m denotes the mass of the peanut oil sample (g), V represents the volume of $Na_2S_2O_3$ consumed by the sample (mL), V_0 refers to the volume of $Na_2S_2O_3$ consumed by the blank experiment (mL), and C stands for the concentration of $Na_2S_2O_3$ (mol/L).

The AV of peanut butter samples was determined in accordance with Chinese National Standard GB 5009.229-2

$$\text{AV (mg / g)} = \frac{\text{(A-B)} \times \text{N} \times 56.1}{\text{W}}$$

Where A is the volume of KOH used for titrating peanut oil (mL), B is the volume of KOH used for titrating the blank (mL), N is the concentration of KOH (mol/L), and W is the mass of the oil (g).

The measurement of TBA value was performed using the method described by Matsushita et al. (2010). Two g of peanut butter was mixed with 10 mL of 7.5% trichloroacetic acid, shaken at room temperature (150 r/min) for 30 min. Five mL of the filtrate was mixed with 5 mL of 0.02 M TBA, heated in a 90 °C water bath for 60 min, then cooled to room temperature and centrifuged (25 °C, 12000 g, 5 min). Absorbance was recorded at 532 nm.

$$\text{TBA (mg / kg)} = \frac{\text{A532}}{\text{W}} \times 9.48$$

Where A_{532} is the absorbance value of the sample solution at 532 nm, and W is the mass of the peanut butter sample (g).

The determination of the total phenolic content (TPC) in peanut butter was performed according to the method of Silva et al. (2022). Specifically, 2 g of peanut butter was added to 10 mL of n-hexane and stirred with a magnetic stirrer for 1 h. The mixture was then centrifuged at 4000 rpm for 10 min at 4 °C, and the supernatant was removed. The defatting process was repeated three times and the sample was blown by nitrogen gas. Next, 1 g of defatted peanut butter was added to 10 mL of 80% ethanol solution and stirred for 1 h. The mixture was then centrifuged at 4000 rpm for 10 min at 4 °C. An aliquot (0.25 mL) of the supernatant was mixed with 2 mL of distilled water and 0.25 mL of Folin-Ciocalteu reagent. The mixture was kept in the dark at room temperature for 3 min, after which 0.25 mL of saturated sodium carbonate solution was added. The samples were then incubated in a 37 °C water bath in darkness. The absorbance was measured at 750 nm using a UV-vis spectrophotometer (UV-6100S, Shanghai Meiboda Instrument Co., Ltd., Shanghai, China). The total phenolic content was calculated using gallic acid as the standard and expressed as milligrams of gallic acid equivalents (GAE) per gram of peanut butter (mg GAE/g).

2.9.3. Fatty acid analysis

The fatty acid composition of peanut butter was analyzed using the method outlined by Wazir et al. (2019). A total of 50 mg of the extracted oil was weighed and dissolved thoroughly in 2 mL of n-hexane, followed by vortex mixing for 1 min to achieve complete homogenization. Subsequently, 1 mL of 0.5 mol/L potassium hydroxide-methanol solution was added, and the mixture was vortexed for 30 s, then heated in a water bath at 60 °C for 10 min with shaking every 2 min to facilitate the conversion of fatty acids into fatty acid methyl esters. Afterward, 1 mL of saturated sodium chloride solution was added and mixed thoroughly to terminate the reaction. Then, 2 mL of n-hexane was added to extract the fatty acid methyl esters, and the mixture was vortexed for 1 min and centrifuged at 4000 r/min for 5 min, followed by standing for stratification. The fatty acid composition was subsequently analyzed using a gas chromatograph, and the fatty acid contents were reported as triglyceride equivalents.

2.9.4. Protein extraction

The peanut butter protein was extracted using a previously described method with minor adjustments (Wanibadullah, 2013). Two grams of peanut butter were combined with 10 mL of chloroform-methanol (2:1, v/v) and shaken for 30 min, then centrifuged (4 °C, 12,000 rpm, 10 min). After twice again centrifugation, the defatted peanut butter powder was then dried under nitrogen for 2 h. Subsequently, 1 g of the dried peanut butter powder was combined with 10 mL of PBS buffer (0.2 M, pH 7.9) and stirred at room temperature (150 rpm, 48 h). The mixture underwent centrifugation (12,000 rpm, 4 °C, 30 min), and the resulting supernatant was vacuum freeze-dried to obtain peanut butter protein. Protein content was determined by Bradford method (Karimi et al., 2022).

2.9.5. Detection of the carbonyl content of protein

The carbonyl content was assessed using the DNPH method (Lenz et al., 1989). Mix 1 mL of protein solution (5 mg/mL) with 1 mL of 10% trichloroacetic acid, react for 2 min, and then centrifuge at 12,000 rpm and 4 °C for 5 min. The pellet was dissolved in 2 mL of 2 M HCl containing 0.2% DNPH and allowed to react for 1 h in the dark at room temperature. Next, 2 mL of 10% trichloroacetic acid was added, and the mixture was centrifuged again at 12,000 rpm, 4 °C, for 5 min. The precipitate was washed three times using a 1:1 ethanol/ethyl acetate solution, then mixed with 3 mL of 6 M guanidine hydrochloride. It was incubated at 37 °C for 60 min, and the absorbance was measured at 370 nm, with a blank sample used as the control. The carbonyl content was calculated as follows:

$$\text{Carbonyls content (mol / L)} = \frac{\text{Abs}_{\text{sample}}}{\varepsilon * l}$$

Where ε represents the molar absorptivity coefficient of 22,000 L/(mol·cm), and l denotes the path length of the cuvette.

2.9.6. Amino acid profile (AAP) analysis

The amino acid of peanut butter was measured in accordance with the method specified in Chinese National Standard GB 5009.124-2016. A total of 50 mg of freeze-dried protein was placed in a hydrolysis tube, to which 10 mL of 6 M HCl and five drops of phenol were subsequently added. After hydrolysis at 110 °C for 22 h, the hydrolysate was adjusted to a final volume of 100 mL with ultrapure water. One milliliter of the hydrolysate was subsequently evaporated to eliminate HCl, after which the residue was mixed with 1 mL of 0.2% sodium citrate solution. Finally, the solution was filtered through a 0.22 μm filter and the amino acid content was quantified using an amino acid analyzer (S-433D, Sykam, Germany).

2.9.7. SDS-PAGE

SDS-PAGE analysis was performed following the protocol by Wanibadullah (2013). The separating gel concentration was 12%, and the stacking gel concentration was 5%. The constant voltage was set at 200 V, and Coomassie Brilliant Blue was introduced to stain the gel. The intensities of the peanut butter protein bands were quantified using ImageJ 2 (Rueden et al., 2017), where the intensity of control-0d (fresh peanut butter) was set as 100%.

2.10. Sensory analysis

The sensory analysis was adapted with slight modifications based on the previously established method (García-Díez et al., 2022). Eight professional assessors (4 males and 4 females, 20-25 years old) were recruited to assess the sensory quality of peanut butter. They have received unified and standardized training to proficiently grasp the definitions, grading criteria and scoring rules for indicators of peanut butter such as color, odor, texture, flavor and mouthfeel. All peanut butter samples were assigned different numbers. Evaluators were instructed to assess the following attributes using a 10-point hedonic scale: Rancid oil flavor, Sour, Roasted nuts, Sweet aroma, Burned taste, Grainy, Spreadability, and Chewiness. A score of 10 represents “Excellent”, while a score of 1 represents “Very Poor”. The average value was calculated from the scoring results.

2.11. Statistical analysis

Each experiment was performed at least three times in triplicate. Results are presented as the mean ± standard deviation (SD). Statistical analyses were conducted using SPSS version 27.0 (IBM, Armonk, NY, USA).

3. Results

3.1. Analysis of GEO components

GC-MS analysis identified a total of 104 compounds in the GEO (extraction rate was 1.72%), including 33 olefins, 26 alcohols, 11 aldehydes, 11 alkanes, 9 esters, 6 ketones, 4 acids, and 4 phenols. Among them, the top 16 compounds are listed in Table 1, with the major constituents being α-zingiberene (25.299%), β-bisabolene (11.826%), β-sesquiterpene (9.368%), 3-ethy1-3-hexene (7.892%), α-curcumene (5.459%), 3,7-dimethyl-2,6-octadienal (4.985%), 2,3-butanediol (4.903%), and citral (3.727%).

3.2. GEO performed antifungal activity against A. flavus

Table 2 illustrates the effect of GEO on the mycelial growth of *A. flavus* in a non-contact manner. After 72 h, the suppression rate of *A. flavus* mycelial growth by GEO at 6 μL/mL was approximately 74.23%. At higher concentrations of GEO (8 and 10 μL/mL), both of the inhibition rates reached 100%. Hence, the MIC of GEO against *A. flavus* was 8 μL/mL.

3.3. GEO blending influenced the characteristics of chitosan films

The chitosan film is light yellow in color, and its transparency decreases upon the addition of GEO (Fig. S1). As GEO exhibits a golden-yellow color, when incorporated into chitosan films, it imparts a progressively yellowish hue to the films as its concentration increases. Table 3 illustrates the physical properties of different films. Firstly, with the rising concentration of GEO, the films exhibited a significant enhancement in thickness (from 0.17 ± 0.00 to 0.23 ± 0.01 mm) ($P < 0.05$). All C-GEO films exhibited lower swelling degree, with the C-GEO3 film achieving the lowest swelling degree of 124.38 ± 15.64%, whereas the chitosan film demonstrated the highest swelling degree of 363.45 ± 15.54%. The chitosan film without GEO exhibited the highest water solubility and moisture content, at 38.23 ± 1.52% and 16.13 ± 0.79%, respectively. In contrast, the addition of GEO resulted in significant reductions in both the water solubility and moisture content of the films. The C-GEO3 film showed the lowest values, with water solubility and moisture content of 18.96 ± 0.68% and 15.84 ± 0.29%, respectively.

3.4. C-GEO films performed promising antioxidant activities

The antioxidant capabilities of GEO composite films were demonstrated via DPPH and ABTS scavenging activities (Fig. 1). Chitosan films exhibited low scavenging activities for DPPH and ABTS of 7.4% and 39.8%, respectively. With the increasing concentration of GEO, the antioxidant activity increased remarkably. In detail, in comparison to chitosan films, for C-GEO3 treated group, the DPPH radical scavenging activity was about 5 times higher (42.3%), while its ABTS radical scavenging ability increased by approximately 2 times (82.1%).

Table 1
Chemical composition of GEO analyzed by GC-MS.

Compound name	Content (%)
α-zingiberene	25.299
β-bisabolene	11.329
β-sesquiphellandrene	9.368
3-ethy1-3-hexene	7.892
α-curcumene	5.459
(E) 3,7-dimethyl-2,6-octadienal	4.958
2,3-butanediol	4.903
Citral	3.727
Pentanol	2.458
2- zinol	1.826
3,7-dimethyl-2,6-octadien-1-ol	1.489
Cyclohexane	1.299
Octanone	1.194
Oleanol	1.022
[1R - (1R *, 4Z, 9S *)] −4,11,11-trimethyl-8-methylene-dicyclo [7.2.0] 4-undeecene	0.99
α-terpineol	0.874

Table 2
Non-contact antifungal activity of GEO on *A. flavus*.

Concentration (μg/mL)	Mycelial growth inhibition (%)		
	24 h	48 h	72 h
0	0.00 ± 0.00^{e}	0.00 ± 0.00^{e}	0.00 ± 0.00^{c}
2	54.24 ± 2.82^{d}	17.12 ± 1.20^{d}	0.00 ± 0.00^{c}
4	79.21 ± 0.24^{c}	52.18 ± 0.67^{c}	32.30 ± 1.32^{c}
6	94.24 ± 3.45^{b}	88.14 ± 0.67^{b}	74.23 ± 1.13^{b}
8	100.00 ± 0.00^{a}	100.00 ± 0.00^{a}	100.00 ± 0.00^{a}
10	100.00 ± 0.00^{a}	100.00 ± 0.00^{a}	100.00 ± 0.00^{a}

Different superscripts (a-e) within the same column indicate statistically significant differences ($P < 0.05$).

3.5. C-GEO films inhibited the growth of A. flavus on peanut butter in a non-contact manner

For the antifungal experiment, Fig. 2 shows that *A. flavus* grows strongly on untreated peanut butter. Without any films, white mycelia almost fully covered the surface after 48 h. Peanut butter with chitosan film also exhibited fungal growth, though it was less than the control. The C-GEO1 film showed minor fungal growth after 72 h. In contrast, the strongest inhibition effects were found for C-GEO2 and C-GEO3 films treated groups, where no mycelial growth was observed.

3.6. C-GEO films influenced texture properties of peanut butter

The texture parameters of peanut butter include hardness, cohesiveness, adhesiveness, and gumminess (Lee & Resurreccion, 2022). As shown in Table 4, after 21 days of storage at 40 °C, the hardness of the control peanut butter significantly increased from 0.82 ± 0.04 N to 0.96 ± 0.14 N ($P < 0.05$), while the hardness of the peanut butter containing chitosan films and C-GEO composite films showed minimal changes. In terms of adhesiveness, the adhesiveness at day 0 was approximately 34.2 N*sec. After 21 days, the control and chitosan film treated groups exhibited the highest adhesiveness values, 93.8 ± 4.45 and 86.1 ± 7.46 N*sec, respectively. Although the adhesiveness of peanut butter treated with C-GEO composite films also increased during storage, the final values were much lower than that of the control-21d, where the lowest value was found for C-GEO3 group (50.8 ± 9.16 N*sec). At the end of storage, the values of cohesiveness and gumminess of C-GEO3 group showed no significant changes compared to those of control-0d.

3.7. C-GEO films changed the color and pH value of peanut butter

During storage, the color of peanut butter changed from yellow-brown to dark brown, with a gradual decrease in brightness. As shown in Fig. 3A & Table S2, the color difference (ΔE) of the control group after 21 days storage was 4.04 ± 0.03, while for the chitosan film group, the value was 3.64 ± 0.28. ΔE values showed a negative correlation with the concentration of incorporated GEO, where the lowest value (1.30 ± 0.14) was observed in the C-GEO3 group. In Fig. 3B & Table S3, the pH values in the control group and the chitosan group decreased slightly from 7.53 ± 0.13 to 6.54 ± 0.07 and 6.60 ± 0.06, respectively, by the end of the storage. While the increasing GEO concentration caused the pH value to decrease more slowly, in the C-GEO3 group, the pH value was 7.04 ± 0.07, which is close to that of control- 0 d.

Table 3
Physical properties of the films.

Parameter	Different films			
	Chitosan	C-GEO1	C-GEO2	C-GEO3
Thickness (mm)	0.17 ± 0.00^{d}	0.19 ± 0.02^{c}	0.20 ± 0.01^{b}	0.23 ± 0.01^{a}
Swelling index (%)	547.78 ± 4.72^{a}	390.49 ± 7.29^{b}	280.01 ± 6.87^{c}	238.71 ± 3.94^{d}
Water solubility (%)	38.23 ± 1.52^{a}	27.89 ± 0.55^{b}	20.42 ± 1.56^{c}	18.96 ± 0.68^{d}
Moisture content (%)	21.69 ± 0.45^{a}	18.95 ± 0.23^{b}	17.83 ± 0.25^{c}	15.84 ± 0.29^{d}

Different superscripts (a-d) within the same row indicate statistically significant differences ($P < 0.05$).

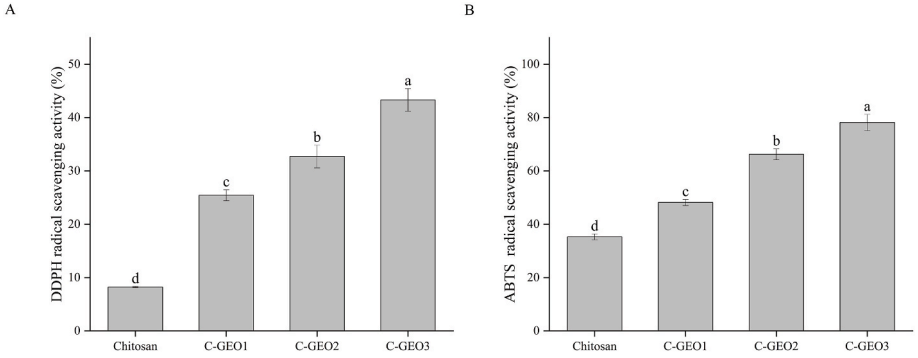

Fig. 1. DPPH (A) and ABTS (B) radical scavenging activity of the films. Chitosan is a chitosan film without ginger essential oil. C-GEO1, C-GEO2, and C-GEO3 are chitosan films containing 0.4%, 0.8%, and 1.6% ginger essential oil, respectively.

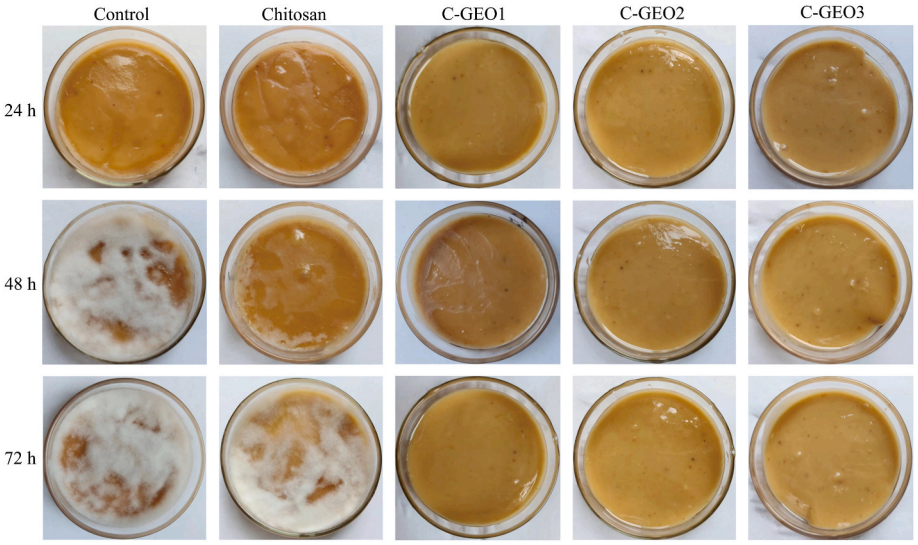

Fig. 2. Non-contact antifungal effect of C-GEO films against *A. flavus* on peanut butter.

Table 4
Effect of the films on the texture of peanut butter stored at 40 °C for 21 days.

	Hardness (N)		Adhesiveness (N*sec)		Cohesiveness		Gumminess	
	0 d	21d	0 d	21d	0 d	21d	0 d	21d
Control	0.82 ± 0.04^{A}	0.96 ± 0.14^{aB}	34.2 ± 4.47^{A}	93.8 ± 4.45^{aB}	0.71 ± 0.03^{A}	0.46 ± 0.03^{dB}	0.21 ± 0.01^{A}	0.28 ± 0.01^{aB}
Chitosan	0.82 ± 0.04^{A}	0.83 ± 0.06^{bA}	34.2 ± 4.47^{A}	86.1 ± 7.46^{bB}	0.71 ± 0.03^{A}	0.50 ± 0.02^{cB}	0.21 ± 0.01^{A}	0.27 ± 0.04^{aB}
C-GEO1	0.82 ± 0.04^{A}	0.83 ± 0.07^{bA}	34.2 ± 4.47^{A}	81.6 ± 8.04^{cB}	0.71 ± 0.03^{A}	0.61 ± 0.02^{bB}	0.21 ± 0.01^{A}	0.25 ± 0.01^{bB}
C-GEO2	0.82 ± 0.04^{A}	0.82 ± 0.01^{bA}	34.2 ± 4.47^{A}	73.8 ± 8.40^{dB}	0.71 ± 0.03^{A}	0.64 ± 0.02^{bB}	0.21 ± 0.01^{A}	0.23 ± 0.02^{cB}
C-GEO3	0.82 ± 0.04^{A}	0.84 ± 0.02^{bA}	34.2 ± 4.47^{A}	50.8 ± 9.16^{eB}	0.71 ± 0.03^{A}	0.69 ± 0.02^{Aa}	0.21 ± 0.01^{A}	0.21 ± 0.03^{dA}

Different superscripts (A-B) indicate statistically significant differences ($P < 0.05$) within the same row. Different superscripts (a-e) indicate statistically significant differences ($P < 0.05$) within the same column.

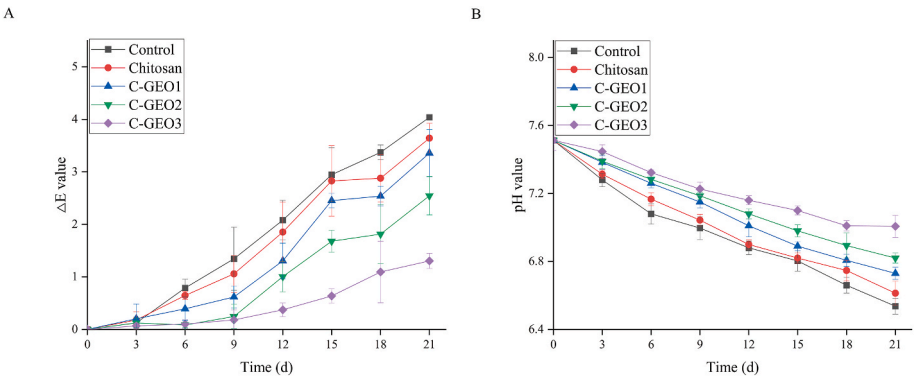

Fig. 3. Effect of the films on the color difference (A) and pH value (B) of peanut butter stored at 40 °C for 21 days.

3.8. C-GEO films effectively delayed the rise in AV, PV, TBARS, while mitigating the decrease in TPC

In Table S1, the peanut butter contains approximately 48.25% lipids. As the primary products of lipid degradation, peroxides can be evaluated with PV, while secondary oxidation products (e.g. 2-hexenal, formaldehyde, acetic acid, etc) can be evaluated by TBARS (Abeyrathne et al., 2021). In addition, AV usually indicates the quantity of free fatty acids. In Fig. 4A & Table S4, freshly made peanut butter contains 0.043 g/100 g of PV. As the storage time prolonged, on 21 d, the PV of peanut butter in the control group and the chitosan group reached 0.319 g/100 g and 0.277 g/100 g, respectively, both exceeding the maximum allowable PV limit of 0.25 g/100 g for peanut butter specified in Chinese national standards (GB5009.227—2016). For the C-GEO treatment groups, the increases in PV values were retarded. Notably, the PV of peanut butter in the C-GEO3 group was only 0.151 g/100 g at the end of storage, demonstrating the strongest inhibition of oxidation. The AV (Fig. 4B & Table S5) and TBA (Fig. 4C & Table S6) values of peanut butter showed a similar trend. At the end of storage, although the PV, AV, and TBA values of peanut butter in all treatment groups increased, the rate of increase in the peanut butter treated with C-GEO films was significantly ($P < 0.05$) slower than that of the control group and the chitosan film group. Peanut butter is inherently rich in polyphenolic compounds. During oxidation, the endogenous polyphenols in peanut butter are preferentially consumed to scavenge free radicals. Consequently, changes in polyphenol content can serve as an indicator of the oxidation degree in peanut butter. Fig. 4D & Table S7 shows that over time, the TPC of peanut butter in the control group and chitosan group decreased from 0.664 mg GAE/g to 0.210 mg GAE/g and 0.318 mg GAE/g, respectively, while the TPCs of peanut butter in the C-GEO1, C-GEO2, and C-GEO3 groups were 0.568, 0.581, and 0.594 mg GAE/g, respectively. The C-GEO films effectively inhibited the decrease in the TPC content of peanut butter.

3.9. C-GEO films preserved the content of free fatty acids

The relative content of individual free fatty acids was determined to decipher which one contributed to the lipid oxidation (Waraho et al.,

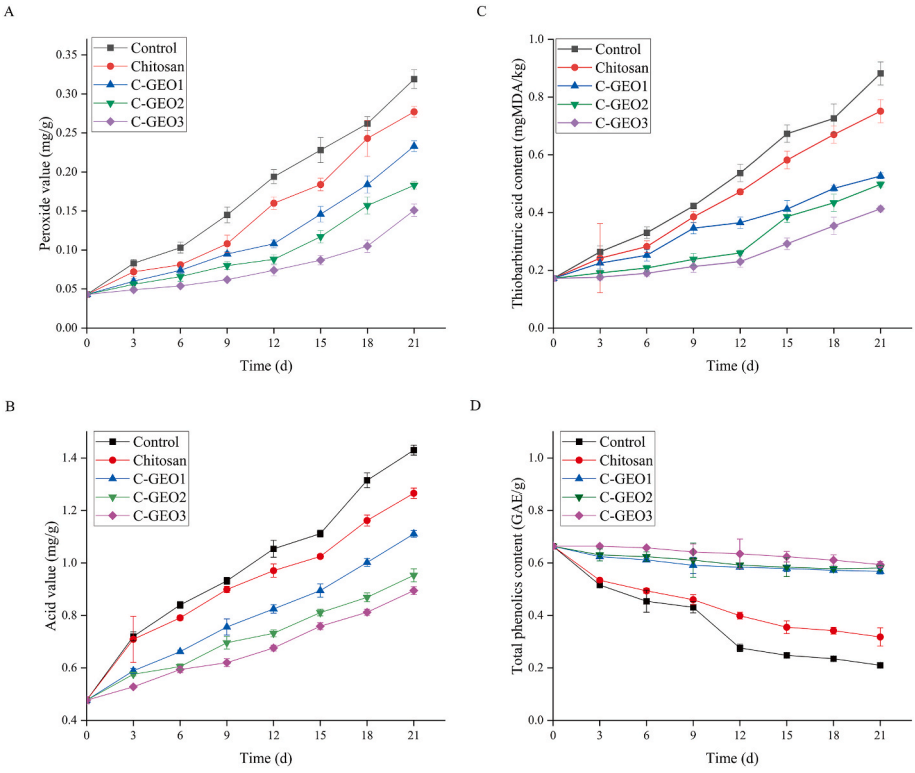

Fig. 4. Influence of C-GEO films on PV (A), AV (B), TBA (C) and TPC (D) of peanut butter samples during storage at 40 °C for 21 days.

2011). As shown in Table 5, by the end of storage, the content of palmitoleic acid and oleic acid in both the control group and chitosan film group significantly decreased compared to fresh peanut butter (control-0 d). For the control group, the decreasing rates of palmitoleic acid and oleic acid were 4.62% and 5.55%, respectively. For the chitosan film group, the decreasing rates of them were 4.28% and 5.67%. For the C-GEO groups, palmitoleic acid also significantly decreased, but it remained significantly higher than that of the control and chitosan groups. Interestingly, the oleic acid content in the three GEO incorporated films treated peanut butter did not change significantly ($P > 0.05$). For the other fatty acids (palmitic acid, stearic acid, arachidic acid, etc.), no significant changes were detected in either control or films treated groups.

3.10. C-GEO films suppressed carbonyl formation

In Table S1, the peanut butter contains approximately 24.90% protein. The principle of protein oxidation is the attack of free radicals on amino acid residues, leading to cleavage or modification of amino acid side chains and ultimately the formation of carbonyl groups (Domínguez et al., 2022). Once formed, carbonyl groups are not easily eliminated by conventional food processing conditions, let alone during food storage. Hence, the accumulated carbonyl content serves as an important indicator of the extent of protein oxidation (Guo et al., 2022; Wu et al., 2024). As depicted in Fig. 5 & Table S8, the carbonyl content of fresh peanut butter was 0.305 nmol/mg. By the end of storage, the carbonyl content increased to 1.285 and 1.165 nmol/mg in the control group and the chitosan film group, respectively. In contrast, the carbonyl content in the C-GEO1, C-GEO2, and C-GEO3 groups increased to 1.032, 0.864, and 0.539 nmol/mg, respectively, where the C-GEO3 can, to the greatest extent, alleviated carbonyl production within 21 days.

3.11. C-GEO films preserved the content of free amino acids

As shown in Table 6, The valine (Val) content in both the control (1.01 ± 0.03 g/100g) and chitosan (1.02 ± 0.06 g/100g) groups decreased significantly after storage compared to the initial value (1.13 ± 0.05 g/100g), while no significant changes were observed in the C-GEO1 (1.10 ± 0.03 g/100g), C-GEO2 (1.10 ± 0.06 g/100g), and C-GEO3 (1.12 ± 0.02 g/100g) groups. For tyrosine (Tyr), the content significantly decreased in the control (0.95 ± 0.01 g/100g), chitosan (0.94 ± 0.06 g/100g), and C-GEO1 (0.95 ± 0.06 g/100g) groups in comparison to the initial value (1.12 ± 0.09 g/100g); however, the C-GEO2 (1.06 ± 0.03 g/100g) and C-GEO3 (1.12 ± 0.09 g/100g) groups showed no significant change. Similarly, phenylalanine (Phe) content was significantly reduced in the control, chitosan, and C-GEO1 groups, remaining the content in the C-GEO2 and C-GEO3 groups unchanged. For the remaining amino acids (e.g., Asp, Thr, Ser, etc.), no significant changes were observed across all groups after 21 days.

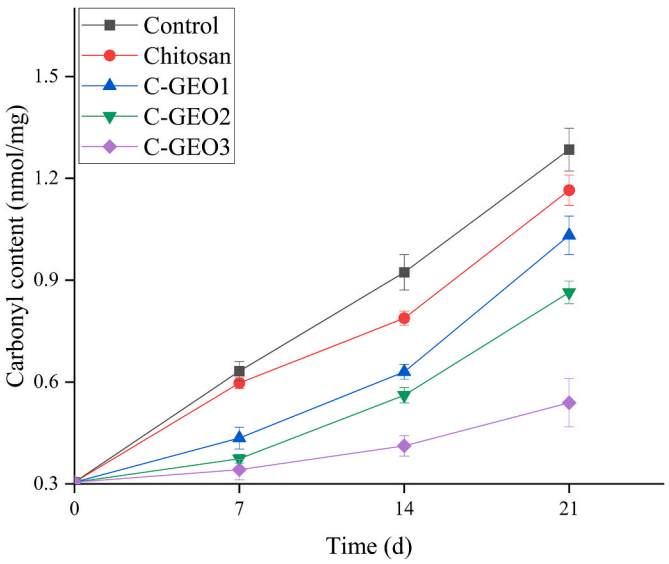

Fig. 5. Influence of C-GEO films on carbonyl content of peanut butter stored at 40 °C for 21 days.

3.12. C-GEO films inhibited protein aggregation and degradation

According to the representative protein subunits in peanut butter, the SDS-PAGE bands are primarily divided into three regions: the conarachin region (66.2 kDa), the acidic conarachin region (43-38 kDa), and the alkaline conarachin region (22.9-18 kDa) (Bianchi-Hall et al., 1993). Fig. 6 & Table S9 show that during storage, by day 7, the conarachin band intensity in the control and chitosan film groups decreased from 100.00% (fresh peanut butter) to 91.40% and 91.78%, respectively. These values further dropped to 76.16% and 76.68% by day 21. In contrast, the conarachin band intensities of C-GEO1, C-GEO2, and C-GEO3 remained at 93.35%, 95.11%, and 97.40% after 21 days of storage, where no significant changes were found in comparison with the fresh sample ($P > 0.05$). For alkaline subunit bands, the control and chitosan film groups showed decreases from 100.00% (fresh) to 81.90% and 83.02% by day 21, whereas C-GEO1, C-GEO2, and C-GEO3 maintained values of 92.21%, 93.72%, and 96.45%, respectively. Similarly, acidic subunit band intensities in the control and chitosan film groups declined from 100.00% to 79.11% and 82.44%, while no significant changes were detected in the C-GEO groups throughout the storage period.

3.13. C-GEO films retained flavor

Peanut butter undergoes rapid sensory deterioration during storage due to lipid oxidation, protein degradation, and flavor loss, with rancidity, spreadability, aroma, and texture serving as key indicators of freshness (Liu et al., 2025). As shown in Fig. 7, the sensory evaluation of

Table 5
Fatty acid analysis of peanut butter stored at 40 °C on day 0 and 21.

Fatty acid (%)	Control-0 d	21 d Free fatty acid content				
		Control	Chitosan	C-GEO1	C-GEO2	C-GEO3
Palmitic acid	10.48 ± 0.58	10.45 ± 0.45	10.40 ± 0.41	10.48 ± 0.05	10.46 ± 0.04	10.45 ± 0.05
Stearic acid	5.01 ± 0.09	5.00 ± 0.03	5.06 ± 0.02	5.07 ± 0.03	5.06 ± 0.05	5.04 ± 0.05
Arachidic acid	1.82 ± 0.05	1.83 ± 0.03	1.83 ± 0.05	1.83 ± 0.07	1.84 ± 0.02	1.85 ± 0.02
Behenic acid	2.49 ± 0.04	2.49 ± 0.04	2.53 ± 0.03	2.49 ± 0.07	2.50 ± 0.02	2.51 ± 0.03
Lignoceric acid	1.03 ± 0.02	1.02 ± 0.03	1.05 ± 0.02	1.05 ± 0.01	1.03 ± 0.05	1.02 ± 0.04
Palmitoleic acid	43.71 ± 2.37^{a}	41.69 ± 2.40^{c}	41.84 ± 2.47^{c}	42.38 ± 0.19^{b}	42.28 ± 0.17^{b}	42.32 ± 0.13^{b}
Oleic acid	34.76 ± 2.95^{a}	32.83 ± 2.83^{b}	32.79 ± 2.77^{b}	34.37 ± 0.06^{a}	34.53 ± 0.03^{a}	34.45 ± 0.07^{a}
Linoleic acid	0.70 ± 0.01	0.70 ± 0.01	0.70 ± 0.01	0.64 ± 0.08	0.68 ± 0.01	0.70 ± 0.02

Different superscripts (a-c) within the same row indicate statistically significant differences ($P < 0.05$).

Table 6
Amino acid analysis of peanut butter treated with C-GEO films at 40 °C for 21 days.

Amino (g/100g)	Control-0 d	21 days amino acid content				
		Control	Chitosan	C-GEO1	C-GEO2	C-GEO3
Asp	3.24 ± 0.02	3.20 ± 0.07	3.18 ± 0.02	3.22 ± 0.05	3.22 ± 0.06	3.22 ± 0.09
Thr	0.73 ± 0.05	0.71 ± 0.37	0.70 ± 0.10	0.72 ± 0.05	0.71 ± 0.01	0.72 ± 0.05
Ser	1.25 ± 0.11	1.20 ± 0.23	1.19 ± 0.20	1.22 ± 0.09	1.22 ± 0.09	1.24 ± 0.13
Glu	5.98 ± 0.47	5.94 ± 0.18	5.95 ± 0.01	5.96 ± 0.09	5.96 ± 0.27	5.95 ± 0.02
Gly	1.59 ± 0.12	1.54 ± 0.06	1.53 ± 0.06	1.57 ± 0.05	1.55 ± 0.06	1.58 ± 0.16
Ala	1.20 ± 0.11	1.19 ± 0.07	1.18 ± 0.03	1.19 ± 0.09	1.19 ± 0.06	1.18 ± 0.15
Cys	0.25 ± 0.02	0.22 ± 0.02	0.21 ± 0.02	0.23 ± 0.03	0.25 ± 0.02	0.22 ± 0.02
Val	1.13 ± 0.05^{a}	1.01 ± 0.03^{b}	1.02 ± 0.06^{b}	1.10 ± 0.03^{a}	1.10 ± 0.06^{a}	1.11 ± 0.02^{a}
Met	0.25 ± 0.02	0.23 ± 0.01	0.22 ± 0.02	0.24 ± 0.02	0.25 ± 0.01	0.22 ± 0.05
Ile	0.88 ± 0.05	0.86 ± 0.05	0.86 ± 0.05	0.86 ± 0.03	0.85 ± 0.03	0.86 ± 0.04
Leu	1.83 ± 0.15	1.77 ± 0.06	1.76 ± 0.05	1.79 ± 0.03	1.79 ± 0.07	1.80 ± 0.09
Tyr	1.12 ± 0.09^{a}	0.95 ± 0.01^{b}	0.94 ± 0.06^{b}	0.95 ± 0.07^{b}	1.06 ± 0.03^{a}	1.12 ± 0.09^{a}
Phe	1.49 ± 0.16^{a}	1.24 ± 0.06^{c}	1.23 ± 0.08^{c}	1.25 ± 0.09^{bc}	1.41 ± 0.05^{abc}	1.44 ± 0.12^{ab}
His	0.85 ± 0.06	0.80 ± 0.03	0.79 ± 0.01	0.81 ± 0.08	0.80 ± 0.02	0.81 ± 0.02
Lys	0.95 ± 0.09	0.88 ± 0.01	0.91 ± 0.03	0.88 ± 0.03	0.89 ± 0.03	0.93 ± 0.04
Arg	3.22 ± 0.27	3.18 ± 0.06	3.17 ± 0.12	3.19 ± 0.13	3.20 ± 0.10	3.20 ± 0.09
Pro	1.49 ± 0.13	1.40 ± 0.04	1.43 ± 0.48	1.41 ± 0.08	1.42 ± 0.10	1.42 ± 0.15

Different superscripts (a-c) within the same row indicate statistically significant differences ($P < 0.05$).

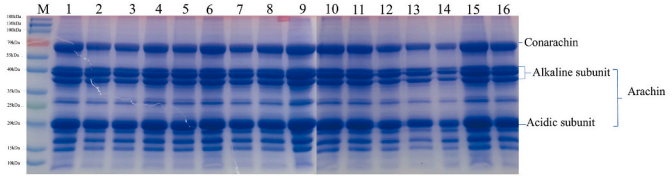

Fig. 6. SDS-PAGE analysis of total soluble proteins in peanut butter stored at 40 °C for 21 days. M: marker; Lane 1 represents fresh peanut butter; lanes 2-6 represent control, chitosan, C-GEO1, C-GEO2 and C-GEO3 treated peanut butter for 7 days, respectively, lanes 7-11 represent control, chitosan, C-GEO1, C-GEO2 and C-GEO3 treated peanut butter for 14 days, lanes 12-16 represent control, chitosan, C-GEO1, C-GEO2 and C-GEO3 treated peanut butter for 21 days.

fresh peanut butter was favorable, with excellent scores in terms of texture and aroma. After 21 days of storage, the control group exhibited a significantly increased rancid flavor, with almost no detectable nutty aroma, rendering it nearly inedible. This indicates that the quality of untreated peanut butter deteriorated heavily during storage at a relatively high temperature. The chitosan group showed some positive effects, but its sensory performance remained unacceptable. Both the control group and the chitosan film group experienced severe lipid deterioration and oil separation after the storage period, resulting in a loss of spreadability. In contrast, in the C-GEO1, C-GEO2, and C-GEO3 groups, as the concentration of GEO increased, rancid flavors decreased, while sensory attributes such as nutty aroma and sweet notes were improved as expected. Notably, sensory properties (sweet aroma, roasted nuts, spreadability, and chewiness) of C-GEO3 were close to those of fresh peanut butter, especially the acceptability level, which was nearly equivalent to that of fresh peanut butter.

4. Discussion

Plant-derived essential oils have garnered interest because of their remarkable antimicrobial efficacy, environmentally friendly nature, low toxicity levels, and high effectiveness (Quinto et al., 2019). However, the volatility and instability of essential oils, along with their strong aromas, often negatively influence the flavor and quality of food products when used directly. Therefore, effectively controlling the release of essential oils, masking their strong aromas, and enhancing their stability has become a critical challenge for their application in food processing and preservation (Liao et al., 2021; Liu et al., 2024). In the present work, to avoid direct contact that might alter the sensory profile of peanut butter, chitosan-ginger essential oil (C-GEO) composite films were physically attached to the inner side of the container lid, functioning as a non-contact, sustained-release active packaging system.

The efficacy of this system is fundamentally governed by the structural reorganization of the film matrix. As the GEO concentration increased, the film thickness increased significantly, while water solubility, swelling index, and moisture content decreased (Table 3). Serving as the primary biopolymer scaffold, chitosan chains, rich in amino ($-NH_2$) and hydroxyl (-OH) groups, form a dense hydrogen-bonding network. Upon the addition of GEO, polar terpenoids (e.g., citral, β-eucalyptol) engage in strong hydrogen bonding with the chitosan

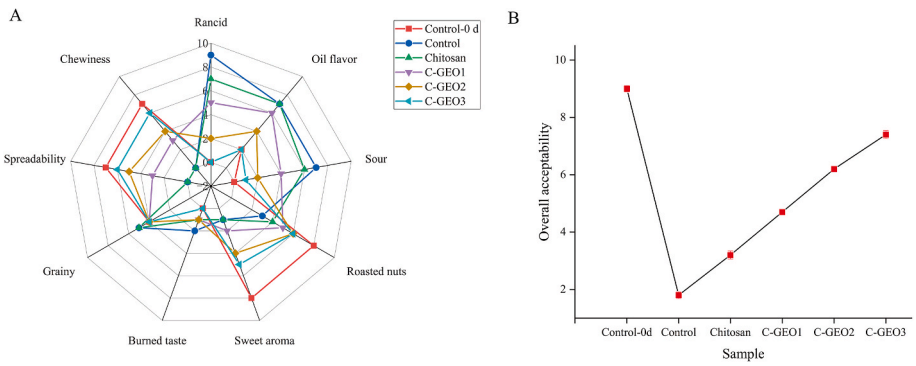

Fig. 7. Sensory evaluation of peanut butter treated with C-GEO stored at 40 °C for 21 days. (A) rancid, oil flavor, sour, roasted nuts, sweet aroma, burned taste, grainy, spreadability and chewiness scores. (B) overall acceptability. Control-0d is the newly produced peanut butter.

chains, while nonpolar components (e.g., α-zingiberene, β-bisabolene) embed into the network via hydrophobic interactions (Al-Hilifi et al., 2022). These cross-scale intermolecular interactions competitively disrupt the pre-existing hydrophilic networks within the original chitosan material, thereby displacing bound water and enhancing the moisture barrier properties (Jahed et al., 2017). Furthermore, hydrophobic association increases the spatial distance between polymer chains, yielding a thicker, labyrinth-like 3D network (Elshamy et al., 2021). More importantly, this structurally modified matrix acts as an internal physical barrier to the encapsulated active compounds. Instead of allowing rapid volatilization, the dense biopolymer network physically retards the diffusion of GEO molecules towards the film surface, ensuring a prolonged and steady vapor-phase release into the packaging headspace.

Facilitated by this controlled release, the vaporized GEO exhibited potent biological activities. In terms of restraining *A. flavus* contamination, GEO possessed a strong inhibitory effect with a MIC of 8 μL/mL. This value is much lower than the MIC of *cinnamomum zeylanicum* blume essential oil (40 μL/mL) (Carmo et al., 2008), though slightly higher than that of peppermint essential oil (0.343 μL/mL) (Yi et al., 2025), confirming GEO's high antifungal potency. When incorporated into chitosan, the composite film continued to exert promising antifungal effects, indicating that the dense network did not trap the active components. The feasibility of utilizing such biopolymer networks for controlled vapor-phase release has been corroborated across various food matrices, ranging from chitosan-pectin-thyme essential oil films on milk cakes (Mulla et al., 2024) and nanocellulose-gellan gum with *Anethum graveolens* essential oil on bread (Sripahco et al., 2023), to chitosan-gelatin with lemongrass essential oil coatings on fresh raspberries (Jovanović et al., 2021) and chitosan-based films incorporated with olive leaves extract on chicken meat (Musella et al., 2021).

The most direct indicators of peanut butter shelf-life deterioration are macroscopic physical changes, particularly texture, color, and pH value, which heavily influence consumer acceptance. During storage, untreated peanut butter exhibited a marked deterioration in texture, characterized by increased hardness and adhesiveness, alongside decreased cohesiveness (Table 4). These rheological changes are driven by complex biochemical alterations at the oil-protein interface. Increased hardness and adhesiveness are primarily attributed to oxidized lipid-mediated surface modification of peanut proteins (arachin and conarachin). Lipid free radicals are supposed to continuously attack the protein interface, exposing buried hydrophobic patches and modifying surface amino acids, which drives protein subunits to reorganise and aggregate into compact networks (Domínguez et al., 2022). Conversely, cohesiveness decreases as oil phase separation weakens internal connectivity (Schaich, 2014). It is worth noting that the composite film significantly modified the internal microenvironment of the packaging. Given the non-contact setup on the inner lid, the pure chitosan film could not function as a traditional external oxygen-blocking wrapping. Instead, its regulatory effect on the microenvironment was purely physical; utilizing the highly hydrophilic nature of chitosan, the film acted as a moisture buffer, passively absorbing trace free moisture from the headspace and moderately lowering the local relative humidity (Aguirre-Loredo et al., 2021). However, this pure physical humidity regulation offered negligible protection against lipid-protein interfacial oxidation. Consequently, pure chitosan only served as a weak physical barrier against environmental oxygen. In contrast, the vapor-phase release of GEO aldehydes and terpenoids intercepted the lipid oxidation chain at the initial stage, protecting protein structural integrity and stabilizing the continuous lipid phase. This structure-preserving capability of essential oil-loaded films is highly universal. Similar textural protection driven by oxidation inhibition was observed by Wang et al. (2020) using apricot kernel essential oil-chitosan films on five-spice beef, and by Venkatachalam et al. (2024) using cinnamon essential oil coatings on tomatoes.

Color darkening, another critical macroscopic defect, arises from a synergy of the Maillard reaction, lipid autoxidation, and protein complexation. Lipid oxidation yields secondary products like short-chain aldehydes and ketones, which possess inherent yellow/brown hues and actively cross-link with proteins to form dark Schiff bases. By acting as potent free radical scavengers, the vapor-phase of C-GEO films suppressed the generation of lipid oxidation products, cutting off carbonyl precursors necessary for lipid-browning. The universality of mitigating abnormal pigmentation via essential oil-mediated radical scavenging is further supported by Khruengsai et al. (2024), who used *Zanthoxylum limonella* essential oil-infused films to preserve the color of pork during storage.

Given that high-temperature roasting effectively inactivates endogenous lipases in peanut butter, the decline in pH value observed in the control group acts as a macroscopic indicator of advanced lipid autoxidation, wherein unsaturated fatty acids are cleaved into short-chain carboxylic acids (e.g., propionic and butyric acids) (Souza et al., 2017). The C-GEO composite films significantly delayed this acidification. This physical protection implies that vapor-phase terpenoids from GEO act as potent free radical scavengers, interrupting the oxidation cascade and reducing the accumulation of acidic byproducts.

To elucidate the fundamental molecular drivers behind the macroscopic deteriorations in texture, color, and pH value, we investigated lipid oxidation profiles. During the 21-day storage, primary (PV) and secondary (AV, TBA) oxidation indicators in the control and pure chitosan groups increased significantly (Fig. 4). Pure chitosan exerted only a slight inhibitory effect, as its physical presence primarily modulated headspace humidity without providing any chemical radical-scavenging capability. Conversely, instead of physically blocking oxygen permeation, the vapor-phase GEO components (e.g., α-zingiberene, α-curcumene) acted as exceptional hydrogen atom donors, rapidly reacting with microenvironmental oxygen species and lipid peroxyl radicals at the interface to terminate chain reactions (Höferl et al., 2019). Although peanut lipids differ compositionally from animal fats, GEO's radical-quenching capability demonstrates broad applicability across food systems. Similar interceptions of primary and secondary lipid oxidation cascades have been well-documented using GEO in meat products, such as apricot kernel essential oil in spiced beef (Wang et al., 2020) and *Artemisia fragrans* essential oil in fresh chicken breast (Yaghoubi et al., 2021). The dynamic equilibrium of quality preservation also involves retaining endogenous bioactive compounds. Polyphenols inherently present in peanuts serve as natural antioxidants but are susceptible to autoxidation and degradation. The continuous supply of exogenous antioxidants from vaporized GEO competitively scavenged reactive oxygen species, protecting peanut polyphenols from radical-induced consumption. This protective effect is consistent with the findings of Venkatachalam et al. (2024) and Montero-Prado et al. (2011), who reported that cinnamon essential oil can protect endogenous phenolic compounds in tomatoes and peaches from oxidation and degradation.

This radical-quenching mechanism is also reflected in the dynamic changes of the fatty acid profile (Table 5). In peanut butter, the saturated to unsaturated fatty acid ratio is approximately 1:3 (Negoita et al., 2018). The content of saturated fatty acids (e.g., palmitic and stearic acids) remained stable across all groups due to the absence of carbon-carbon double bonds (C=C), granting them high chemical inertia against free radical abstraction. Similar results were also observed in crude palm oil, refined palm oil, palm oil extract, and palm stearin; the high content of saturated fatty acids in these samples contributed to their low degree of oxidation over the 12-month storage period (Almeida et al., 2019).

Conversely, unsaturated fatty acids (palmitoleic and oleic acids) served as primary targets for oxidative degradation. The allylic hydrogens adjacent to their C=C double bonds exhibit low electron density and are easily abstracted by ROS (Ding et al., 2022). In the control group, the significant decline in these acids indicates massive auto-oxidative cleavage, where palmitoleic acid is oxidized into

α,β-unsaturated aldehydes (Gao et al., 2023), and oleic acid is oxidized to form octanal, nonanal, decanal, 2-decenal and 2-undecenal (Cao et al., 2020). Overall total fatty acids also decreased due to the formation of high-molecular-weight dimers and trimers via polymerization (Boisset et al., 2024). By saturating the headspace with electron-rich terpenoids, C-GEO films effectively shielded these allylic hydrogens. The vulnerability of these specific unsaturated fatty acids and the necessity of antioxidant intervention well align with findings by Safaei et al. (2024) and Mohebpour et al. (2023), who demonstrated that incorporating phenolic-rich date paste or encapsulated peanut skin extracts effectively shielded oleic and linoleic acids from oxidative cleavage in peanut-based matrices.

In high-fat matrices, lipid and protein oxidation are tightly coupled. Secondary metabolites of lipid oxidation, particularly reactive carbonyls, serve as bridges transferring oxidative damage to proteins. Carbonyl content is therefore recognized as a coupled indicator reflecting both lipid oxidation intensity and amino acid damage (Geng et al., 2023). During storage, the carbonyl content in the control group increased dramatically. However, the increasing rate in the C-GEO groups was significantly suppressed, indicating that GEO successfully blocked the downstream propagation of oxidation to the protein phase. The principle of preventing protein oxidation by interrupting lipid-derived carbonyl generation has been corroborated using cinnamon essential oil and nutmeg essential oil to smoked beef (Afidah, 2022).

This interrupted cascade directly protected specific susceptible amino acids (Table 6). While cysteine, methionine, and histidine remained relatively stable initially, a pronounced decrease in tyrosine (Tyr), phenylalanine (Phe), and valine (Val) occurred in the control and pure chitosan groups within 3 weeks. Tyr and Phe possess electron-rich aromatic rings highly susceptible to electrophilic radical attack (e.g., •OH oxidizing tyrosine to dopaquinone) (Hellwig, 2020). The valine side chain contains a branched alkyl group, and hydrogen abstraction from its β-position exhibits the lowest energy barrier among the direct hydrogen-atom transfer pathways, rendering this site a preferential target for hydroxyl radical attack (Chan et al., 2018). Interestingly, Wanibadullah (2013) found that in Ready-to-Eat packaged peanut butter stored at 40 °C, these sensitive amino acids remained stable for the first 3 weeks before declining. The earlier onset of degradation in our control group may stem from differences in packaging oxygen permeability and endogenous radical fluxes. Nonetheless, by scavenging •OH radicals in the vapor phase, C-GEO films effectively shielded these vulnerable amino acids. Similar targeted protection of Tyr, Phe, and Val against oxidative cleavage was reported by Santos et al. (2019) using a mixed essential oil (eucalyptol/carvacrol/thymol) in fish meat, contrasting sharply with the severe degradation of tyrosine and serine observed under high-flux oxidative stress, such as electron-beam irradiated peanut butter (El-Rawas et al., 2012).

The protection of individual amino acids ultimately dictates macromolecular protein integrity (Lu et al., 2024), visualized through SDS-PAGE profiling. In the control group, the band intensities of arachin (66.2 kDa) and conarachin acidic subunits (43 kDa) significantly faded. This indicates severe oxidative degradation and the conversion of soluble proteins into insoluble aggregates via extensive carbonylation cross-linking, similar to soy proteins (Guo et al., 2022). Wanibadullah (2013) observed only limited dissociation of peanut protein subunits, possibly due to strict anaerobic MRE conditions limiting carbonylation. In our aerobic system, relying solely on the physical barrier of pure chitosan was insufficient. In contrast, C-GEO3 band intensities remained highly comparable to fresh peanut butter. By neutralizing reactive carbonyls, the sustained release of GEO prevented the abnormal covalent assembly of protein subunits. This molecular-level preservation of protein integrity via antioxidant-active packaging is consistent with findings in ferulic acid & rutin-treated yak beef (Li et al., 2022) and rosemary/oregano essential oil-incorporated pork patties (Nieto et al., 2013), and fundamentally explains why the peanut butter retained its original macroscopic texture.

Finally, consumer acceptance remains the ultimate criterion for evaluating food preservation strategies. By employing a non-contact design, C-GEO composite films decoupled the preservation function from direct matrix contamination. The controlled release of GEO provided a subtle, fresh herbaceous fragrance to the headspace, masking trace odors of lipid autoxidation without overpowering the characteristic roasted peanut flavor. The overall acceptance scores confirmed that this non-contact strategy harmonizes robust physiochemical preservation (antimicrobial, lipid/protein oxidation inhibition) with excellent organoleptic quality, presenting a highly viable technological approach for extending the shelf life of high-fat, high-protein food systems.

Despite these promising findings, the present study has certain limitations. First, the specific dynamic release kinetics of GEO into the packaging headspace were not quantified; future research should characterize the release profiles under fluctuating practical conditions. Second, the long-term partitioning behavior of volatile compounds into the high-fat peanut butter matrix requires further quantitative analysis. Lastly, the efficacy of C-GEO films against a broader spectrum of spoilage microorganisms needs validation for practical commercial scale-up.

5. Conclusion

Incorporating GEO into chitosan films in a non-contact manner has shown remarkable antifungal efficacy against *A. flavus* and strong influence in maintaining the quality of peanut butter during storage. The presence of GEO led to significant changes in the physical properties of the film, enhancing its thickness, hydrophobicity, and antioxidant activity. In addition, C-GEO films preserved the texture, color, and pH value of peanut butter, delayed lipid and protein oxidation and maintained its sensory stability. Notably, the promising effects of composite films are indeed the synergistic functions of essential oil and chitosan film integrating chemical activities (e.g. antioxidant & antimicrobial properties) with physical barrier (e.g. water retention, oxygen barrier, and structural support). This functional complementarity creates a multifunctional system that provides superior protective performance, far exceeding the limitations of pure physical barriers. Future studies will aim to elucidate the molecular mechanisms of GEO against *A. flavus*, model its volatile release kinetics, and evaluate the scale-up feasibility of these non-contact systems for industrial application.

CRediT authorship contribution statement

Yiming Zhang: Writing – original draft, Methodology, Data curation. **Qian Li:** Writing – review & editing, Supervision, Resources, Conceptualization. **Fred Mwabulili:** Investigation. **Hongying Xiao:** Writing – original draft. **Jianhua Wang:** Supervision.

Ethical approval

Ethical approval was not necessary for this study.

Declaration of competing interest

The authors declare that they have no known competing financial interests or personal relationships that could have appeared to influence the work reported in this paper.

Acknowledgments

The authors declare financial support was received for the research, authorship, and/or publication of this article. We thank for the financial support of National Key R&D Program of China (2025YFF1107604-03), Henan Province Key Research and Development and promotion Project (Science and Technology Research) (252102110078), Cultivation

Programme for Young Backbone Teachers in Henan University of Technology (0503/21421231), Research Fund of Henan University of Technology (076H2024LY076, 388H2024LY388, and 389H2024LY389), and Double First-Class Discipline Construction Program of Henan University of Technology (0517-24410014).

Appendix A. Supplementary data

Supplementary data to this article can be found online at https://doi.org/10.1016/j.lwt.2026.119500.

Data availability

Data will be made available on request.

References

Abeyrathne, E. D. N. S., Nam, K., & Ahn, D. U. (2021). Analytical methods for lipid oxidation and antioxidant capacity in food systems. *Antioxidants, 10*(10), 1587–1606. https://doi.org/10.3390/antiox10101587

Afidah, U. (2022). *Effect of cinnamon and nutmeg essential oils on the smoked meat (Se'i Sapi) quality. Master of science in food science and technology*. Bangkok, Thailand: Chulalongkorn University.

Aguirre-Loredo, R. Y., Velazquez, G., Guadarrama-Lezama, A. Y., et al. (2021). Water adsorption thermodynamical analysis and mechanical characterization of chitosan and polyvinyl alcohol-based films. *Journal of Polymers and the Environment, 30*(5), 1880–1892. https://doi.org/10.1007/s10924-021-02316-x

Akyuz, L., Kaya, M., Ilk, S., et al. (2018). Effect of different animal fat and plant oil additives on physicochemical, mechanical, antimicrobial and antioxidant properties of chitosan films. *International Journal of Biological Macromolecules, 111*(1), 475–484. https://doi.org/10.1016/j.ijbiomac.2018.01.045

Al-Hilifi, S. A., Al-Ali, R. M., & Petkoska, A. T. (2022). Ginger essential oil as an active addition to composite chitosan films: Development and characterization. *Gels, 8*(6), 327–341. https://doi.org/10.3390/gels8060327

Almeida, D. T.d., Viana, T. V., Costa, M. M., et al. (2019). Effects of different storage conditions on the oxidative stability of crude and refined palm oil, olein and stearin (*Elaeis guineensis*). *Food Science and Technology, 39*(1), 211–217. https://doi.org/10.1590/fst.43317

Balaguer, M. P., Lopez-Carballo, G., Catala, R., et al. (2013). Antifungal properties of gliadin films incorporating cinnamaldehyde and application in active food packaging of bread and cheese spread foodstuffs. *International Journal of Food Microbiology, 166*(3), 369–377. https://doi.org/10.1016/j.ijfoodmicro.2013.08.012

Bianchi-Hall, C. M., Keys, R. D., Stalker, H. T., et al. (1993). Diversity of seed storage protein patterns in wild peanut (*Arachis, Fabaceae*) species. *Plant Systematics and Evolution, 186*(1), 1–15. https://doi.org/10.1007/bf00937710

Boisset, L., Pascale, d. C., Stojmilovic, I., et al. (2024). Monitoring lipid oxidation in multiple emulsions by near infrared spectroscopy. *European Journal of Lipid Science and Technology, 126*(6), 1–9. https://doi.org/10.1002/ejlt.202300267

Brewer, M. S. (2011). Natural antioxidants: Sources, compounds, mechanisms of action, and potential applications. *Comprehensive Reviews in Food Science and Food Safety, 10*(4), 221–247. https://doi.org/10.1111/j.1541-4337.2011.00156.x

Burt, S. (2004). Essential oils: Their antibacterial properties and potential applications in foods—a review. *International Journal of Food Microbiology, 94*(3), 223–253. https://doi.org/10.1016/j.ijfoodmicro.2004.03.022

Calderón-Oliver, M., & Ponce-Alquicira, E. (2022). The role of microencapsulation in food application. *Molecules, 27*(5), 1499–1515. https://doi.org/10.3390/molecules27051499

Cao, J., Jiang, X., Chen, Q., et al. (2020). Oxidative stabilities of olive and camellia oils: Possible mechanism of aldehydes formation in oleic acid triglyceride at high temperature. *Lebensmittel-Wissenschaft und -Technologie, 118*(1), Article 108858. https://doi.org/10.1016/j.lwt.2019.108858

Carmo, S. E., Lima, E.d. O., Souza, E. L.d., et al. (2008). Effect of *cinnamomum zeylanicum* blume essential oil on the growth and morphogenesis of some potentially pathogenic. *Brazilian Journal of Microbiology, 39*(26), 91–97. https://doi.org/10.1590/S1517-83822008001000021

Chan, B., Easton, C. J., & Radom, L. (2018). Effect of hydrogen bonding and partial deprotonation on the oxidation of peptides. *The Journal of Physical Chemistry A, 122*(6), 1741–1746. https://doi.org/10.1021/acs.jpca.7b11797

Chen, P., Yang, Q., Zhang, L., et al. (2024). Ginger essential oil extracted by low-temperature continuous phase transition and its preservation effect on prepared duck meat. *Food and Bioprocess Technology, 18*(3), 2806–2819. https://doi.org/10.1007/s11947-024-03643-2

Ding, C., Wang, L., Yao, Y., et al. (2022). Mechanism of the initial oxidation of monounsaturated fatty acids. *Food Chemistry, 392*(30), Article 133298. https://doi.org/10.1016/j.foodchem.2022.133298

Domínguez, R., Pateiro, M., Munekata, P. E. S., et al. (2022). Protein oxidation in muscle foods: A comprehensive review. *Antioxidants, 11*(1), 60–84. https://doi.org/10.3390/antiox11010060

El-Rawas, A., Hvizdzak, A., Davenport, M., et al. (2012). Effect of electron beam irradiation on quality indicators of peanut butter over a storage period. *Food Chemistry, 133*(1), 212–219. https://doi.org/10.1016/j.foodchem.2011.12.078

Elshamy, S., Khadizatul, K., Uemura, K., et al. (2021). Chitosan-based film incorporated with essential oil nanoemulsion foreseeing enhanced antimicrobial effect. *Journal of Food Science and Technology, 58*(9), 3314–3327. https://doi.org/10.1007/s13197-020-04888-3

Gao, P., Bao, Y., Wang, S., et al. (2023). Mechanism of palmitoleic acid oxidation into volatile compounds during heating. *Flavour and Fragrance Journal, 38*(2), 95–107. https://doi.org/10.1002/ffj.3728

García-Díez, E., Sánchez-Ayora, H., Blanch, M., et al. (2022). Exploring a cocoa–carob blend as a functional food with decreased bitterness: Characterization and sensory analysis. *Lebensmittel-Wissenschaft und -Technologie, 165*(1), Article 113708. https://doi.org/10.1016/j.lwt.2022.113708

Geng, L., Liu, K., & Zhang, H. (2023). Lipid oxidation in foods and its implications on proteins. *Frontiers in Nutrition, 10*(11), Article 1192199. https://doi.org/10.3389/fnut.2023.1192199

Gong, A., Shi, A., Liu, H., et al. (2018). Relationship of chemical properties of different peanut varieties to peanut butter storage stability. *Journal of Integrative Agriculture, 17*(5), 1003–1010. https://doi.org/10.1016/s2095-3119(18)61919-7

Guo, Y., Wang, Z., Hu, Z., et al. (2022). The temporal evolution mechanism of structure and function of oxidized soy protein aggregates. *Food Chemistry X, 15*(1), Article 100382. https://doi.org/10.1016/j.fochx.2022.100382

Hamad, A., Djalil, A. D., & Hartanti, D. (2023). Galangal and ginger essential oils exerted microbial growth inhibitory activity and preservation potential on tofu. *Food Research, 7*(1), 27–34. https://doi.org/10.26656/fr.2017.7(S1).7

Hellwig, M. (2020). Analysis of protein oxidation in food and feed products. *Journal of Agricultural and Food Chemistry, 68*(46), 12870–12885. https://doi.org/10.1021/acs.jafc.0c00711

Höferl, M., Stoilova, I., Wanner, J., et al. (2019). Composition and comprehensive antioxidant activity of ginger (*Zingiber officinale*) essential oil from Ecuador. *Natural Product Communications, 10*(6), 1085–1090. https://doi.org/10.1177/1934578x1501000672

Huang, Z., Guo, B., Deng, C., et al. (2020). Stabilization of peanut butter by rice bran wax. *Journal of Food Science, 85*(6), 1793–1798. https://doi.org/10.1111/1750-3841.15176

IndexBox. (2026). China - Peanut butter and prepared or preserved groundnuts - Market analysis, forecast, size, trends and insight, from. https://www.indexbox.io/store/china-peanut-butter-and-prepared-or-preserved-groundnuts-market-analysis-forecast-size-trends-and-insights/.

Jahed, E., Khaledabad, M. A., Almasi, H., et al. (2017). Physicochemical properties of *Carum copticum* essential oil loaded chitosan films containing organic nanoreinforcements. *Carbohydrate Polymers, 164*(1), 325–338. https://doi.org/10.1016/j.carbpol.2017.02.022

Jovanović, J., Ćirković, J., Radojković, A., et al. (2021). Chitosan and pectin-based films and coatings with active components for application in antimicrobial food packaging. *Progress in Organic Coatings, 158*(10), Article 106349. https://doi.org/10.1016/j.porgcoat.2021.106349

Karimi, F., Hamidian, Y., Behrouzifar, F., et al. (2022). An applicable method for extraction of whole seeds protein and its determination through Bradford's method. *Food and Chemical Toxicology, 164*(1), Article 113053. https://doi.org/10.1016/j.fct.2022.113053

Khruengsai, S., Phoopanasaeng, P., Sripahco, T., et al. (2024). Application of chitosan films incorporated with *Zanthoxylum limonella* essential oil for extending shelf life of pork. *International Journal of Biological Macromolecules, 262*(1), Article 129703. https://doi.org/10.1016/j.ijbiomac.2024.129703

Knutsen, H. K., Alexander, J., Barregård, L., et al. (2018). Effect on public health of a possible increase of the maximum level for 'aflatoxin total' from 4 to 10 μg/kg in peanuts and processed products thereof, intended for direct human consumption or use as an ingredient in foodstuffs. *EFSA Journal, 16*(2), Article 025175. https://doi.org/10.2903/j.efsa.2018.5175

Lee, C. M., & Resurreccion, A. V. A. (2022). Improved correlation between sensory and instrumental measurement of peanut butter texture. *Journal of Food Science, 67*(5), 1939–1949. https://doi.org/10.1111/j.1365-2621.2002.tb08750.x

Lenz, A. G., Costabel, U., Shaltiel, S., et al. (1989). Determination of carbonyl groups in oxidatively modified proteins by reduction with tritiated sodium borohydride. *Analytical Biochemistry, 177*(2), 419–425. https://doi.org/10.1016/0003-2697(89)90077-8

Li, S., Tang, S., Li, J., et al. (2022). Protective effects of four natural antioxidants on hydroxyl radical induced lipid and protein oxidation in yak meat. *Foods, 11*(19), 3062–3076. https://doi.org/10.3390/foods11193062

Li, Q., Zhu, X., Xie, Y., et al. (2021). o-Vanillin, a promising antifungal agent, inhibits *Aspergillus flavus* by disrupting the integrity of cell walls and cell membranes. *Applied Microbiology and Biotechnology, 105*(12), 5147–5158. https://doi.org/10.1007/s00253-021-11371-2

Liao, W., Badri, W., Dumas, E., et al. (2021). Nanoencapsulation of essential oils as natural food antimicrobial agents: An overview. *Applied Sciences, 11*(13), 5778–5802. https://doi.org/10.3390/app11135778

Liu, Z., Wang, S., Liang, H., et al. (2024). A review of advancements in chitosan-essential oil composite films: Better and sustainable food preservation with biodegradable packaging. *International Journal of Biological Macromolecules, 274*(1), 133242–133255. https://doi.org/10.1016/j.ijbiomac.2024.133242

Liu, X., Zhu, X., Han, Z., et al. (2025). Recent advances in the mechanisms of quality degradation and control technologies for peanut butter: A literature review. *Foods, 14*(1), 105–131. https://doi.org/10.3390/foods14010105

Lu, C., Zhao, Y., Shi, Q., et al. (2024). Preservation effects of photodynamic inactivation-mediated antibacterial film on storage quality of salmon fillets: Insights into protein quality. *Food Chemistry, 444*(1), Article 138685. https://doi.org/10.1016/j.foodchem.2024.138685

Matsushita, T., Inoue, S., & Tanaka, R. (2010). An assay method for determining the total lipid content of fish meat using a 2-thiobarbituric acid reaction. *Journal of the American Oil Chemists' Society, 87*(9), 963–972. https://doi.org/10.1007/s11746-010-1578-x

Mohebpour, D. A., Dean, L. L., Harding, R. O., et al. (2023). Effect of peanut skin extracts on the shelf life of unstabilized peanut butter. *Peanut Science, 50*(1), 8–21. https://doi.org/10.3146/0095-3679-501-ps22-8

Montero-Prado, P., Rodriguez-Lafuente, A., & Nerin, C. (2011). Active label-based packaging to extend the shelf-life of "Calanda" peach fruit: Changes in fruit quality and enzymatic activity. *Postharvest Biology and Technology, 60*(3), 211–219. https://doi.org/10.1016/j.postharvbio.2011.01.008

Moreno, J. P. (2015). Benefits of a snacking intervention as part of a school-based obesity intervention for Mexican American children. *Journal of Applied Research on Children: Informing Policy for Children at Risk, 6*(2), 1–16. https://doi.org/10.58464/2155-5834.1257

Mulla, M. F. Z., Ahmed, J., Vahora, A., et al. (2024). Characterization of biopolymers based antibacterial films enriched with thyme essential oil and their application for milk cake preservation. *Frontiers in Food Science and Technology, 4*(1), Article 125225. https://doi.org/10.3389/frfst.2024.1356582

Mungalpara, B., Ratanpara, K., Dora, H. K., et al. (2025). Modified atmosphere packaging and its: A review. *International Journal of Science and Technology, 16*(1), 1–13. https://doi.org/10.1080/10408398.2013.862202

Musella, E., Ouazzani, I. C.e., Mendes, A. R., et al. (2021). Preparation and characterization of bioactive chitosan-based films incorporated with olive leaves extract for food packaging applications. *Coatings, 11*(11), 1339–1353. https://doi.org/10.3390/coatings11111339

Negoita, M., Mihai, A. L., Adascalului, A., et al. (2018). Comparison of the fatty acid composition of peanut butter by applying different fat extraction procedures. *Revista de Chimie, 69*(11), 3023–3032. https://doi.org/10.37358/rc.18.11.6675

Nerilo, S. B., Rocha, G. H. O., Tomoike, C., et al. (2015). Antifungal properties and inhibitory effects upon aflatoxin production by *Zingiber officinale* essential oil in *Aspergillus flavus*. *International Journal of Food Science and Technology, 51*(2), 286–292. https://doi.org/10.1111/ijfs.12950

Nerilo, S. B., Romoli, J. C. Z., Nakasugi, L. P., et al. (2020). Antifungal activity and inhibition of aflatoxins production by *Zingiber officinale* Roscoe essential oil against *Aspergillus flavus* in stored maize grains. *Ciência Rural, 50*(6), 1–8. https://doi.org/10.1590/0103-8478cr20190779

Nieto, G., Jongberg, S., Andersen, M. L., et al. (2013). Thiol oxidation and protein cross-link formation during chill storage of pork patties added essential oil of oregano, rosemary, or garlic. *Meat Science, 95*(2), 177–184. https://doi.org/10.1016/j.meatsci.2013.05.016

Quinto, E. J., Caro, I., Villalobos-Delgado, L. H., et al. (2019). Food safety through natural antimicrobials. *Antibiotics, 8*(4), 208–238. https://doi.org/10.3390/antibiotics8040208

Riaz, A., Lei, S., Akhtar, H. M. S., et al. (2018). Preparation and characterization of chitosan-based antimicrobial active food packaging film incorporated with apple peel polyphenols. *International Journal of Biological Macromolecules, 114*(1), 547–555. https://doi.org/10.1016/j.ijbiomac.2018.03.126

Rueden, C. T., Schindelin, J., Hiner, M. C., et al. (2017). ImageJ2 ImageJ for the next generation of scientific image data. *BMC Bioinformatics, 529*(19), 1–26. https://doi.org/10.1186/s12859-017-1934-z

Safaei, S. F., Jafarian, S., Masoumi, M., et al. (2024). Assessment of rheological, qualitative and antioxidant characteristics of enriched peanut butter with date paste through shelf-life stability. *Heliyon, 10*(18), Article e37602. https://doi.org/10.1016/j.heliyon.2024.e37602

Sana, S. S., Gangadhar, L., Sofi, M. A., et al. (2025). Chitosan as a wall biomaterial for the encapsulation of essential oils: A comprehensive review of pharmaceutical breakthroughs and future directions. *International Journal of Biological Macromolecules, 332*(1), Article 148551. https://doi.org/10.1016/j.ijbiomac.2025.148551

Santos, H. M. C., Méndez, L., Secci, G., et al. (2019). Pathway-oriented action of dietary essential oils to prevent muscle protein oxidation and texture deterioration of farmed rainbow trout. *Animal, 13*(9), 2080–2091. https://doi.org/10.1017/s1751731119000016

Saricaoglu, F. T., & Turhan, S. (2019). Performance of mechanically deboned chicken meat protein coatings containing thyme or clove essential oil for storage quality improvement of beef sucuks. *Meat Science, 158*(1), Article 107912. https://doi.org/10.1016/j.meatsci.2019.107912

Schaich, K. M. (2014). Lipid co oxidation of protein one size does not fit all. *INFORM, 1*(1), Article 02088. https://doi.org/10.7554/elife.02088

Septama, A. W., Monika, A. C., Monika, Gabriel, T., et al. (2023). Essential oil of *Zingiber cassumunar* roxb. and *Zingiber officinale* rosc.: A comparative study on chemical constituents, antibacterial activity, biofilm formation, and inhibition of *Pseudomonas aeruginosa* quorum sensing system. *Chemistry and Biodiversity, 20*(6). https://doi.org/10.1002/cbdv.202201205

Shetta, A., Ali, I. H., Sharaf, N. S., et al. (2024). Review of strategic methods for encapsulating essential oils into chitosan nanosystems and their applications. *International Journal of Biological Macromolecules, 259*(1), Article 129212. https://doi.org/10.1016/j.ijbiomac.2024.129212

Showkat, S., Anjum, N., Ayaz, Q., et al. (2025). Enhancing shelflife of plum fruit by chitosan-based nanoemulsion coating incorporated with ginger essential oil. *Applied Food Research, 5*(1), Article 100768. https://doi.org/10.1016/j.afres.2025.100768

Silva, M. P., Martelli-Tosi, M., Massarioli, A. P., et al. (2022). Co-encapsulation of guaraná extracts and probiotics increases probiotic survivability and simultaneously delivers bioactive compounds in simulated gastrointestinal fluids. *Lebensmittel-Wissenschaft und -Technologie, 161*(1), Article 113351. https://doi.org/10.1016/j.lwt.2022.113351

Silva, M. P., Tulini, F. L., Marinho, J. F. U., et al. (2017). Semisweet chocolate as a vehicle for the probiotics Lactobacillus acidophilus LA3 and Bifidobacterium animalis subsp. lactis BLC1: Evaluation of chocolate stability and probiotic survival under in vitro simulated gastrointestinal conditions. *Lebensmittel-Wissenschaft und -Technologie, 75*(1), 640–647. https://doi.org/10.1016/j.lwt.2016.10.025

Sithole, T. R., Ma, Y., Qin, Z., et al. (2022). Peanut butter food safety concerns—prevalence, mitigation and control of salmonella spp., and aflatoxins in peanut butter. *Foods, 11*(13), 1874–1896. https://doi.org/10.3390/foods11131874

Souza, P. T., Ansolin, M., Batista, E. A. C., et al. (2017). Kinetic of the formation of short-chain carboxylic acids during the induced oxidation of different lipid samples using ion chromatography. *Fuel, 199*, 239–247. https://doi.org/10.1016/j.fuel.2017.02.093

Souza, V., Pires, J., Vieira, É., et al. (2018). Shelf life assessment of fresh poultry meat packaged in novel bionanocomposite of chitosan/montmorillonite incorporated with ginger essential oil. *Coatings, 8*(5), 177–194. https://doi.org/10.3390/coatings8050177

Sripahco, T., Khruengsai, S., & Pripdeevech, P. (2023). Biodegradable antifungal films from nanocellulose-gellan gum incorporated with *Anethum graveolens* essential oil for bread packaging. *International Journal of Biological Macromolecules, 243*(1), Article 125244. https://doi.org/10.1016/j.ijbiomac.2023.125244

Sultan, M., Abdelhakim, A. A., Nassar, M., et al. (2023). Active packaging of chitosan film modified with basil oil encapsulated in silica nanoparticles as an alternate for plastic packaging materials. *Food Bioscience, 51*(1), Article 102298. https://doi.org/10.1016/j.fbio.2022.102298

Venkatachalam, K., Lekjing, S., Noonim, P., et al. (2024). Extension of quality and shelf life of tomatoes using chitosan coating incorporated with cinnamon oil. *Foods, 13*(7), 1000–1019. https://doi.org/10.3390/foods13071000

Vitalini, S., Nalbone, L., Bernardi, C., et al. (2022). Ginger and parsley essential oils: Chemical composition, antimicrobial activity, and evaluation of their application in cheese preservation. *Natural Product Research, 37*(16), 2742–2747. https://doi.org/10.1080/14786419.2022.2125965

Wang, D., Dong, Y., Chen, X., et al. (2020). Incorporation of apricot (*Prunus armeniaca*) kernel essential oil into chitosan films displaying antimicrobial effect against *Listeria monocytogenes* and improving quality indices of spiced beef. *International Journal of Biological Macromolecules, 162*, 838–844. https://doi.org/10.1016/j.ijbiomac.2020.06.220

Wanibadullah, W. (2013). *Lipid protein interactions in peanut butter*. New Jersey, New Brunswick, New Jersey: The State University of. Doctoral, Rutgers.

Waraho, T., McClements, D. J., & Decker, E. A. (2011). Impact of free fatty acid concentration and structure on lipid oxidation in oil-in-water emulsions. *Food Chemistry, 129*(3), 854–859. https://doi.org/10.1016/j.foodchem.2011.05.034

Wazir, H., Chay, S. Y., Zarei, M., et al. (2019). Effects of storage time and temperature on lipid oxidation and protein co-oxidation of low-moisture shredded meat products. *Antioxidants, 8*(10), 486–503. https://doi.org/10.3390/antiox8100486

Wu, J., Ji, Y., Xue, J., et al. (2024). Protein oxidation-induced changes in the physicochemical properties and quality of plant food. *International Journal of Food Science and Technology, 59*(6), 3537–3544. https://doi.org/10.1111/ijfs.17135

Yaghoubi, M., Ayaseh, A., Alirezalu, K., et al. (2021). Effect of chitosan coating incorporated with *Artemisia fragrans* essential oil on fresh chicken meat during refrigerated storage. *Polymers, 13*(5), 716–730. https://doi.org/10.3390/polym13050716

Yamamoto-Ribeiro, M. M. G., Grespan, R., Kohiyama, C. Y., et al. (2013). Effect of *Zingiber officinale* essential oil on *Fusarium verticillioides* and fumonisin production. *Food Chemistry, 141*(3), 3147–3152. https://doi.org/10.1016/j.foodchem.2013.05.144

Yi, Y., Liu, R., Shang, Z., et al. (2025). Peppermint essential oil for controlling *Aspergillus flavus* and analysis of its antifungal action mode. *Current Microbiology, 82*(4), 140–150. https://doi.org/10.1007/s00284-025-04116-1

Zhang, X., Liu, J., Yong, H., et al. (2020). Development of antioxidant and antimicrobial packaging films based on chitosan and mangosteen (*Garcinia mangostana* L.) rind powder. *International Journal of Biological Macromolecules, 145*(1), 1129–1139. https://doi.org/10.1016/j.ijbiomac.2019.10.038

Zhu, J., Chen, X., Huang, T., et al. (2022). Characterization and antioxidant properties of chitosan/ethyl-vanillin edible films produced via schiff-base reaction. *Food Science and Biotechnology, 32*(2), 157–167. https://doi.org/10.1007/s10068-022-01178-w